Journal of Membrane Science 610 (2020) 118277

Contents lists available at ScienceDirect

Journal of Membrane Science

journal homepage: http://www.elsevier.com/locate/memsci

Defect free hollow fiber reverse osmosis membranes by combining layer-by-layer and interfacial polymerization

Türkan Ormanci-Acar [a,b], Mehrdad Mohammadifakhr [a], Nieck E. Benes [a], Wiebe M. de Vos [a,*]

[a] Membrane Science and Technology, MESA+ Institute for Nanotechnology, University of Twente, P.O. Box 217, 7500 AE, Enschede, the Netherlands
[b] Istanbul University-Cerrahpaşa, Faculty of Engineering, Department of Environmental Engineering, 34320, Avcılar, Istanbul, Turkey

ARTICLE INFO

Keywords:
Low pressure-reverse osmosis
Polyelectrolytes
Interfacial polymerization
Layer by layer coating
Defect free membranes
Hollow fiber
Micropollutant removal

ABSTRACT

Hollow fibre RO membranes would be desired for many applications, but are notoriously difficult to fabricate. Here we demonstrate that combining layer-by-layer and interfacial polymerization (IP) allows straightforeward production of defect-free hollow fiber RO membranes. A polyelectrolyte multilayer (PEM) is used to fill the pores of a support membrane, to provide a controlled and smooth surface that can nevertheless act as an IP monomer reservoir. This approach is first demonstrated on a model surface, with IP layers being successfully applied on both poly(diallyldimethylammonium chloride) (PDADMAC)/poly(4-styrene sulfonate) (PSS) and poly(ethyleneimine) (PEI)/PSS PEMs. On plain hollow fiber support membranes, IP coating was found to have a success rate as low as 40%. However, by application of a PEM interlayer the success rate increases to 72% for PDADMAC/PSS and 90% for PEI/PSS. Also the separation performance of the successfully prepared IP membranes was significantly better when a PEM interlayer was applied, with higher NaCl retentions (from 94% to 97%), and better removal of organic micro-pollutants (from 96% to 98%), with just a small decrease in permeability (from 0.9 L/m^{2}hbar to 0.7 L/m^{2}hbar). Combining layer-by-layer and IP approaches can thus lead to the fabrication of defect free RO membranes with improved separation performance.

1. Introduction

Water scarcity is one of the major problems to be faced by today's society. Global water usage has increased by as much as six times over the past 100 years [1], and the demand for fresh water is only expected to further increase due to increases in population, economic development and consumption [2]. At the same time, water pollution due to small toxic substances originating from human activity has also seen a strong increase. Numerous new chemicals, compounds and their by-products, here referred to as micropollutants (MPs), are now frequently found in drinking water sources [3].

Many organic micropollutants have been placed on the watch list of the European Union as emerging contaminants and should be actively monitored [4]. Micropollutants found in drinking water sources originate from industrial, medicinal, and agricultural activities, and, they can be toxic to the environment and to humans [5–8]. Because of their small size (between 100 and 1000 Da.), they are difficult to remove using conventional water purification approaches. Dense membrane approaches, such as Nanofiltration (NF) or Reverse Osmosis (RO), have been successful with RO yielding the highest MP retentions [9].

Generally, commercial RO membranes are fabricated as thin film composite (TFC) polyamide membranes. TFC based RO membranes have an ultrathin selective layer that is typically prepared through interfacial polymerization of trimesoyl chloride (TMC) in the organic phase and m-phenilanediamine (MPD) in the aqueous phase on top of a porous support [10]. Due to the fast reaction rate and reasonable solubility of MPD in organic phase, interfacial polymerization (IP) occurs in the organic phase and proceeds by MPD diffusion from aqueous phase to the organic phase. This leads to the growth of a defect free thin film that limits additional monomer diffusion [11]. This multi-staged IP process typically results in the formation of a relatively rough (ridge and valley structure) nonhomogeneous surface [12], with excellent selectivities [9].

A downside of the IP approach is that it works well for flat sheet membranes, while its application for hollow fiber based membranes is notoriously difficult. The hollow shape of membranes complicates homogeneous application of the two monomers, removal of excess solutions and drying process etc., especially when using a conventional TFC

* Corresponding author. Membrane Science and Technology, MESA+ Institute for Nanotechnology, University of Twente, P.O. Box 217, 7500 AE, Enschede, the Netherlands.
E-mail address: w.m.devos@utwente.nl (W.M. de Vos).

https://doi.org/10.1016/j.memsci.2020.118277
Received 25 January 2020; Received in revised form 14 April 2020; Accepted 15 May 2020
Available online 26 May 2020

procedure. This is important as for flat sheet (spiral wound) membranes it is becoming increasingly clear that spacer fouling is a much more substantial problem than fouling of the membrane itself [13]. Hollow fiber membrane modules do not require spacers and would thus show substantially less fouling issues. Clearly, it becomes important to develop a new fabrication method for RO membranes to allow easy fabrication of hollow fiber RO membranes.

Due to the described difficulties, only very limited work has been reported one the fabrication of polyamide hollow fiber reverse osmosis (HF RO) membranes. Zhang, Y., et al., applied zwitterionic copolymers onto a polyamide membrane surface to fabricate a polyamide HF RO membrane. By using that copolymer, they reduced the thickness of the polyamide layer achieved higher permeabilities [14]. In another study [15], polydopamine modified metal organic frameworks (MOFs) were incorporated in polyamide (PA) matrix supported for brackish water desalination in low-pressure reverse osmosis (RO) process. They obtained a relatively high water flux, but an increasing content of MOFs in the membrane caused decrease in the rejection. While both works demonstrate that HF RO is possible, their approaches were certainly not straightforward.

Implementing layer by layer assembly as an interlayer on a porous support before IP step can be an alternative approach for the fabrication of superior RO membranes with independent control over thickness, roughness and chemical functionality. Moreover, it could improve the lumen surface properties to increase the interfacial polymerization success rate. Water-soluble polyelectrolytes have been used for LbL assembly, and they initially go into the pores and after sufficient coating steps block them [16]. Indeed, flatter surfaces with smaller pores can lead to smoother and thinner IP surface coatings for better performing RO membranes [17].

Only a few studies have been performed on combining LbL and IP approaches, all to prepare flat sheet RO membranes. Gu et al. reported that making an interlayer by using LbL assembly enabled the creation of a defect free selective layer with minimal roughness, achieving improved permselectivity and enhanced antifouling performance compared to traditional IP membranes [18]. Also in their second paper, they confirmed that using PEI/PAA based interlayers, smoother and more uniform IP layers could be formed, which they attributed to the uniform distribution of their surface carboxyl groups [19]. By another research group, a 2.5 times higher water flux was found by using PEMs as an interlayer prior to IP compared to conventional IP membranes [20,21].

In this work we propose that using a PEM coating as an interlayer can do more than just improve control over the IP process, it will also allow the fabrication of highly desired hollow fiber RO membranes. Hollow fiber RO membranes would circumvent the problem of spacer fouling but normally they suffer from defects that are detrimental to their separation performance. With the increased control provided by the interlayer, defects would be less likely to occur. Moreover, the interlayer would act similar to a "gutter layer" in dense gas separation membranes, where defects, such as pinholes, are prevented from dominating the separation performance by a less selective layer that is defect free. In this work, we first study the growth of an IP layer on various PEMs on model surfaces to better understand the effect of an interlayer on IP coating. Subsequently, we study the separation properties of hollow fiber RO membranes prepared with and without the presence of a PEM interlayer. We will show that the defect free hollow fiber RO membranes can be prepared, with excellent properties for the removal of micropollutants from drinking water.

2. Materials and methods

2.1. Materials

Poly (diallyl dimethyl ammonium chloride) (PDADMAC, Mw = 150 kDa,20 wt% in water) was obtained from Kemira (Finland). Polystyrene sulfonic acid (PSS, Mw = 100 kDa, 20 wt% in water) was obtained from Tosoh Organic Chemical Co., LTD (Japan). Polyethylenimine, branched (average Mw ~25,000 by LS, average Mn ~10,000 by GPC) was obtained from Sigma-Aldrich. These water soluble polymers were used to coat for layer-by-layer (LbL) assembly on silicon wafers and hollow fiber membranes. For the thin film composite coating, anhydrous n-hexane (≥99.0%), m-phenylenediamine (MPD) flakes, 99% and 1,3,5-Benzenetricarbonyl trichloride (TMC) 98% monomers were obtained from Sigma-Aldrich. All other chemicals were purchased from Sigma-Aldrich and were used without further purification.

Hollow fiber membranes were obtained from NX Filtration B.V. (Enschede, the Netherlands) and are based on sulfonated poly(ether sulfone) and PDADMAC. The fibers are asymmetrical from the inside out, and have a positive surface charge, an inner diameter of 0.68 mm, a MWCO of 25 kDa. Silicon wafers were purchased from WaferNet Inc. (San Jose, USA).

2.2. Reflectometry

Reflectometry was used to study polyelectrolyte multilayer (PEM) growth on silicon wafers. Reflectometry is a sensitive technique to observe the alternating adsorption of different polyelectrolytes on flat, reflective surfaces [22]. Polymer solutions of 0.1 g/L (in this study, PDADMAC and PEI polymer used as cationic polymers, and PSS was used as anionic polymer) with an ionic strength of 0.5 M NaCl were prepared and alternatively adsorbed at room temperature on a silicon wafer with a 75 nm SiO_2 top layer. In between each polyelectrolyte adsorption step, a rinsing step with a background solution (0.5 M NaCl) was applied. In reflectometry, polarized monochromatic light (He–Ne laser, 632.8 nm) hits the wafer around the Brewster angle (71°) and is reflected toward the detector. The reflected light is split into its p- and s-polarized components. The ratio between the change in these components (ΔS) is directly proportional to the amount of mass adsorbed to the wafer, according to Eq. (1) [23]:

$$\Gamma = \frac{\Delta S}{S_0} Q \tag{1}$$

where Γ is the amount of mass adsorbed on the wafer (mg.m^{-2}) and S_0 is the starting output signal of the bare silicon wafer (−). Q is a sensitivity factor, which depends on the angle of incidence of the laser(θ), the refractive indices(n), the thicknesses(d) of the layers on the silicon wafer, and the refractive index increment (dn/dc) of the adsorbate. To calculate the Q-factor an optical model was used, based on the following values: θ = 71°, n_{silica} = 1.46, $\tilde{n}_{silicon}$ = (3.85, 0.02), n_{H2O} = 1.33, $dn/dc_{PDADMAC}$ = 0.18 mL/g, dn/dc_{PSS} = 0.18 mL/g, dn/dc_{PEI} = 0.189 mL/g, d_{silica} = 75 nm [24]. The calculated Q factor (PDADMAC/PSS) = 30 mg m^{-2} and Q factor (PEI/PSS) = 28 mg m^{-2}.

2.3. Ellipsometry

Ellipsometry is a non-destructive optical technique in which the sample to be characterized is illuminated with a beam of polarized light. Ellipsometry measures the change in polarization state of the measurement beam induced by reflection from (or transmission through) the sample. The change in polarization state is commonly characterized by the ellipsometric Psi (Ψ) and Delta (Δ) parameters defined in Eq. (2):

$$\tan \Psi . e^{i\Delta} = \rho = \frac{r_p}{r_s} \tag{2}$$

In this equation, rho (ρ) is defined as the ratio of the reflectivity for p-polarized light (rp) divided by the reflectivity for s-polarized light (rs). ρ is a complex number, and the ellipsometric parameters simply report this value in polar form: tan(Ψ) is the magnitude of the reflectivity ratio, and Δ is the phase.

In this paper, Ellipsometry (Woollam Spectroscopic Ellipsometer) was used to measure the thickness of LbL layers and polyamide layers

(PA) on a reflective silicon wafer.

2.4. LbL assembly and IP coating on model surfaces

Layer by layer (LbL) deposition on an O_2 plasma treated silicon wafer, as a model surface, was performed via a dip coating technique. For dip coating 0.1 g/L polymer solutions were prepared with 0.5 M NaCl. At a higher ionic strength like 0.5 M NaCl, the mobility of polyelectrolytes during PEM formation increases. This results in quick PEM growth and a more open PEM structure both desired properties for our PEM interlayer [16]. First, silicon wafers were immersed in a cationic polymer solution (PDADMAC or PEI) for 15 min, and then immersed in an anionic solution (PSS) for 15 min. Between cationic and anionic polymer solutions, silicon wafers were immersed in a 0.5 M NaCl solution for 5 min. After completing the adsorption of a cationic and an anionic polymer, 1 bilayer was obtained. This procedure was repeated until the desired amount of bilayers was obtained. After coating, silicon wafers were rinsed with deionized water a few times, to remove any unbound polymer and/or salts.

To implement interfacial polymerization (IP) on a silicon wafer, PEM layers were used as an interlayer. For thin film composite (TFC) coating via IP, the aqueous phase solution was prepared by dissolving 2% w/w MPD in deionized water and the organic phase solution was prepared with a 0.1%, w/v TMC in n-hexane at room temperature. The PEM deposited silicon wafer was firstly dipped into the aqueous phase solution and allowed to soak for 2 min. Following the elimination of the excess solution from the coated surface with pressurized air, the aqueous-phase solution saturated silicon wafer was immersed into the organic-phase solution for 1 min. After removing the excess organic solution by washing with n-hexane, the silicon wafer was cured in an oven at 70 °C for 5 min to attain the desired stability of the formed structure.

2.5. LbL assembly and IP coating of hollow fiber membranes

Polyethersulphone (PES) hollow fiber (HF) membranes that contain a first adsorbed layer of the cationic polymer PDADMAC were used as support membranes.

To deposit PEM layers, PDADMAC coated bare membranes were first immersed in a negatively charged polymer solution (0.1 g/l 0.5 M NaCl) solution, for 15 min. Then they were immersed in 3 rinsing solutions (0.5 M NaCl solutions) for 5 min, before immersion in a positively charged polymer solution (0.1 g/l 0.5 M NaCl). After completing the deposition of one layer of anionic and one layer of cationic polymer, a single bilayer was obtained. This procedure was repeated until the desired amount of bilayers was obtained. At the end of coating, HFs were rinsed with deionized water a few times to remove unbound polymers and NaCl. Before preparing HF modules for further steps, all HF membranes were stored in 15% glycerol to avoid the collapse of pores.

After LbL deposition, approximately 23 cm long hollow fiber modules were prepared for interfacial polymerization. One fiber was placed and glued into the 23 cm long tube and Festo pushin-t connector was sticked at the end of two side of tube. A photo of prepared fibers is illustrated in Supplementary Fig. S1. For interfacial polymerization, 2% w/w MPD and 0.1% w/v TMC were used to prepare aqueous and organic solutions, respectively. Before coating, the module was dried with N_2 at each side (lumen and shell) of the membrane (the module has 4 inlets). The MPD solution was applied by using a syringe pump for 5 min, to the lumen surface of the hollow fiber. To remove the excess of MPD solution, the lumen of fiber was dried with N_2 for 3 min, and then a TMC solution was pumped into lumen of fiber for 5 min. After coating, 30 s of N_2 flushing and 30 mL deionized water flushing followed, and a 15 min heat treatment was applied to the coated membranes at 70 °C. After TFC coating, the membranes were stored in deionized water for further experiments.

The steps of LbL assembly and interfacial polymerization are summarized schematically in Fig. 1.

2.6. Membrane characterization and salt retention

Filtration experiments were performed by using a cross flow filtration set up (Cross flow velocity (CFV) for setup was calculated as 0.29 m/s) under an applied pressure of 5 bars. The filtration set up is given in Supplementary Fig. S2. The permeate was collected in a baker and it measured before and after filtration to calculate the permeability. Pure water permeability (PWP) of PEMs coated fiber, PWP and salt retention of thin film composite coated modules were performed by using that set up. For the salt retention experiments, 5 mM NaCl, $CaCl_2$ and Na_2SO_4 solutions were prepared and measured separately. The salt concentrations of the retentate and permeate were measured with a WTW Cond 3210 conductivity meter. The retention was calculated as the ratio between permeate and concentrate concentrations. No significant changes in permeability were observed during filtration.

Surface and cross sectional morphology of all fabricated hollow fibers (before and after IP coating) were investigated with scanning electron micrographs (JEOL JSM-710 field emission scanning electron microscope (FE-SEM)). Samples were coated with a 10 nm chromium layer (Quorum Q150T ES) prior to imaging. Cross-sectional samples were cut after immersing in liquid nitrogen.

2.7. Micropollutants analysis

The molecular weight of the studied MPs ranges between 200 and 650 g/mol. The selection of MPs was made as it contains neutral, positive, and negative molecules at the pH of measurement (pH 5.8) (Table 1). MPs were selected to provide nice overview properties of currently well-known MPs. According to Directive 2008/105/EC, only 33 of MPs's maximum allowable concentrations were listed. Out of used MPs cocktail, only Atrazine is listed there, and it should be lower than 2 μg/L. A micropollutant mix was prepared using 10 mg/L concentrations for each of them. The MPs mix was filtrated at 5 bars through the prepared modules for at least 24 h to ensure steady state retention before collecting samples. The feed and permeate samples were measured by using Dionex Ultimate 3000 U-HPLC system equipped with an RS variable wavelength detector. Micropollutant separation was done on an Acclaim RSLC C18 2.2 μm column (Thermo Scientific) at 65 °C, while applying a gradient flow from 95 wt % H_2O + 5 wt % acetonitrile at pH 4 to 5 wt % H_2O + 95 wt % acetonitrile at 1 mL/min. No significant changes in permeability were observed during filtration.

3. Results and discussion

3.1. Layer deposition on model surfaces

To demonstrate that interfacial polymerization (IP) layers can be successfully prepared on polyelectrolyte multilayer (PEM) layers, we initially studied layer deposition on silicon oxide model surfaces (SiO_2). Ellipsometry was employed to measure the thickness of PEM and IP coatings [25], while we varied the effect of the PEM coating thickness. The refractive index was measured for thick coatings (>30 nm) and subsequently used as an input parameter when modeling the thin coatings. To accurately measure the thickness of an applied IP layer on top of a PEM coating, a 2-layered model was used to determine the thickness of the IP layer. The PEM coatings were always characterized by Ellipsometry before IP coating, and the obtained thicknesses were used as input for the PEM coating in the 2-layered model.

To study the growth of the PEM coatings as a function of the number of deposited bi-layers, silicon wafers were coated from 1 bl to 7 bl (Fig. 2). As expected a systematic increment in the thickness for both polyelectrolyte combinations (PEI/PSS and PDADMAC/PSS) is observed while the number of bilayers increased. For PEI/PSS the growth is relatively linear, with every bi-layer leading to the same increase in

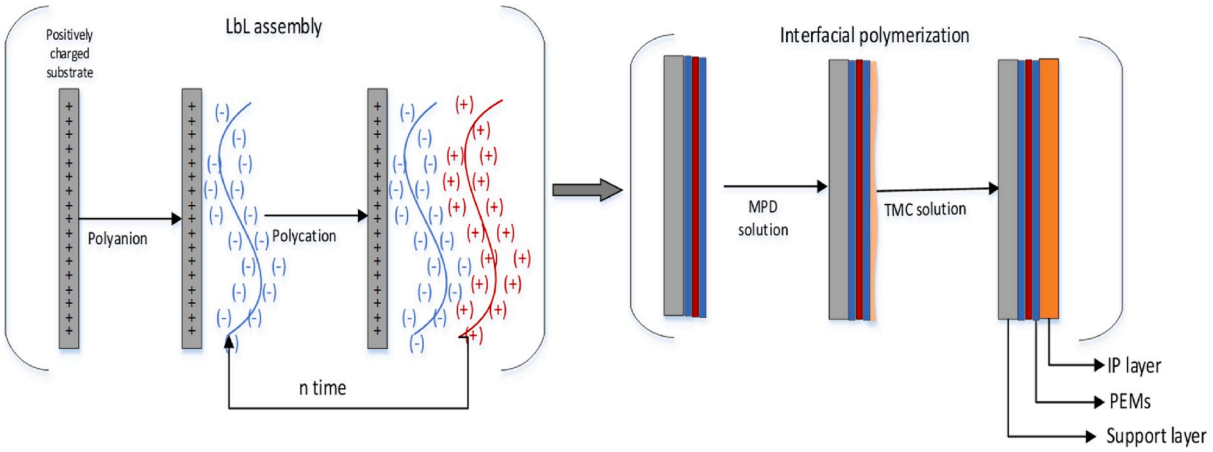

Fig. 1. Schematic diagram of combining layer by layer assembly (LbL) and interfacial polymerization (IP).

Table 1
Properties of the eight micropollutants selected for this study (http://www.chemicalize.org).

MPs	pK_a	Log P	M_r (g/mol)	Charge (pH5.8)
Atenolol	9.7	0.43	266.3	(+)
Atrazine	3.2	2.2	215.7	(0)
Bisphenol A	10.1	4.0	228.3	(0)
Phenolphtalein	9.16	4.4	318.3	(0)
Bromothymol blue	8.41	9.2	624.4	(0)
Sulfamethoxazole	2.0/7.7	0.79	253.3	(0/-)
Naproxen	4.2	3.0	230.3	(−)
Bezafibrate	3.8	4.0	361.8	(−)

thickness, while for PDADMAC/PSS a more exponential growth is observed. At the used high salt concentration of 0.5 M, the mobility of polymer chains, especially PDADMAC becomes quite high, leading to a the exponential growth curve for PDADMAC/PSS [26]. These same growth patterns were also observed by a complementary approach, reflectometry, as shown in Supplementary Fig. S3. Low MSE values were obtained, except for higher thicknesses. Thicker PEM coatings can become rough, leading to a lower correlation between experiment and the used optical model. The thickness PEM coatings varied between 7.6 ± 0.3 nm and 31.0 ± 0.3 nm for PEI/PSS, and 4.6 ± 0.1 nm and 69.3 ± 0.4 nm, for PDADMAC and PSS.

Here we report the PEM dry layer thicknesses, while when exposed to water the PEM will be significantly swollen, especially the outer polyelectrolyte layer. We expect that the swollen outer layer will allow a significant amine uptake. The thicknesses of these applied IP coatings were measured with ellipsometry and are given in Fig. 3 as a function of the PEM thickness in bi-layers. If we examine the thickness of the IP layers on PDADMAC/PSS PEMs, we find a relatively stable thickness of 6–7 nm, which is slightly higher than on PEI/PSS PEMs which show stable thicknesses around 5 nm (at least up to 5 bi-layers). These results immediately show that it is possible to successfully apply IP layers on these PEM coatings, even leading to very thin IP layers. The small difference in thickness between PDADMAC/PSS and PEI/PSS could stem from slightly different interactions between the coatings and the chemicals used in IP coating. For example, PEI can react with TMC while PDADMAC cannot, while also the coating roughness and the contact angle for water and hexane will be different for the two systems. For both PDADMAC/PSS and PEI/PSS, we do observe that for more bi-layers (6 and 7) a somewhat thicker layer is formed. This could be originated from the increased surface roughness of PEM layers. Still, these roughnesses also make it more difficult to get accurate data from ellipsometry and thus high MSE values were found especially for PDADMAC/PSS.

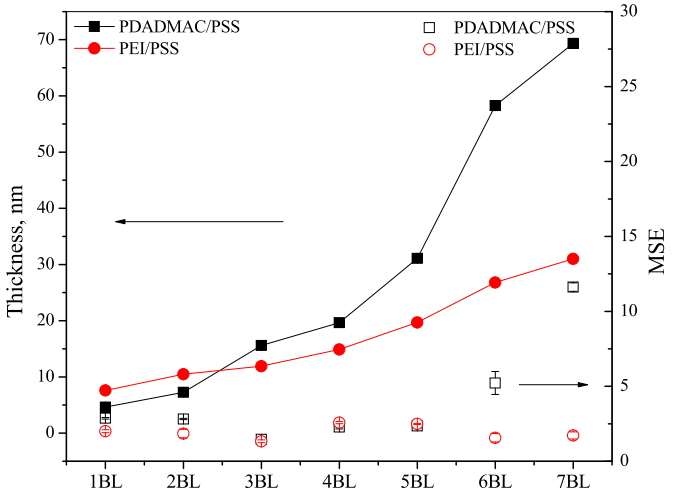

Fig. 2. The thickness of PEM layers as a function of the number of applied bi-layers. The thicknesses were obtained by ellipsometry, and the MSE of the fit is also provided. Lines and filled symbols represent thickness, while open symbols represent MSE's. Experiments were repeated multiple times on at least two separately prepared surfaces. Error bars represent the standard deviation.

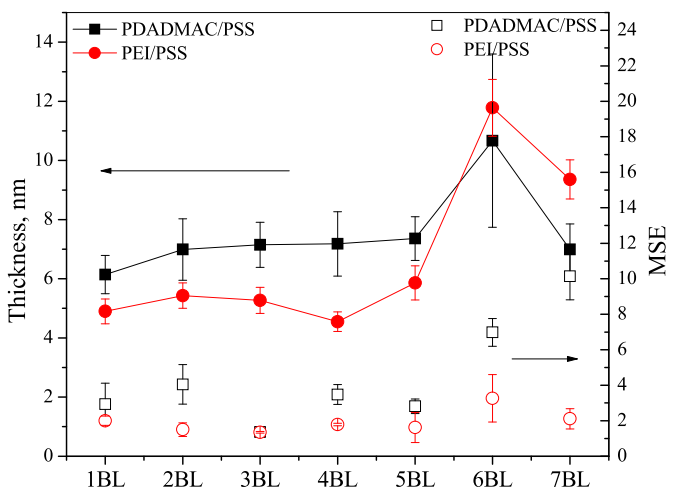

Fig. 3. The thickness of IP layers, prepared on top of PEM coatings as indicated. The measurements were obtained by ellipsometry, and the MSE of the fit is also provided. Lines and filled symbols represent thickness, while open symbols represent MSE's. Experiments were repeated multiple times on at least two separately prepared surfaces. Error bars represent the standard deviation.

"Here we report the dry layer thickness, while when exposed to water the PEM will be significantly swollen, especially the outer polyelectrolyte layer. The swollen outer layer will allow a significant amine uptake."

As the thickness and the type of the PEM interlayer did not affect the thickness of IP layer dramatically and the thickness of the IP layer was found quite thin (around 5–7 nm), it can be said that the PEM surface determines the IP layer thickness. Even 1 polyelectrolyte bilayer was enough to allow successful deposition of an IP coating, something not possible on an uncoated silicon wafer. Based on these promising results we started to apply this combination of PEM and IP coating to hollow fiber membranes. We chose to use PEM coatings of 3.5 bi-layers in thickness as this is thick enough to fill the pore of the membrane support, but thin enough to be in the regime where stable IP thicknesses were observed. We stress that 3.5 bi-layers on top of our positively charged membranes is equal to 4 bi-layers on the negatively charged model surfaces.

3.2. Success rates for the fabrication of hollow fiber RO membranes

The preparation of hollow fiber based RO membranes is notoriously difficult, with defects being a common occurrence. Such defects can be identified by studying the membrane selectivity, with defects leading to membranes with poor retentions. We studied the NaCl retention for membranes prepared with and without a PEM interlayer. This included a membrane coated with just a single layer of polyelectrolyte, as this gives the membrane the same surface chemistry as the PEM interlayer systems, but without filling the membrane pores. For each type of interlayer, at least 10 hollow fiber RO membranes were produced in as individual. Obtained membranes were comparised other polyamide HF RO membranes in the literature in Table 2. Apllying PEM layers prior to interfacial polymerization increased the retention of membranes up to 97% as the permeability of membranes decreased in small quantities. Low pressured Filmtech XLE thin film composite membrane is generally used to removesome inorganic contaminant [27], micropollutants [28], pecticides [29] and other contaminants from water. Dolar D. et al. measured salt performance of Filmtech XLE membrane with 300 ppm feed solution at 25 bar, and they obtained 96.8% retention of NaCl with the permeation of 2.69 ± 0.25. In this study, 97% of NaCl retention was achieved even lower feed solution and lower operation pressure. However, Zang Y., et al. [14] and Lin Y., et al. [15] found higher removal efficiency 98.1% and 97.6%, but higher feed concentrations and higher permeability then this study. But they did not mentioned the reproducibility of fibers which is very hard to do.

Here, a larger than 90% NaCl retention was chosen as an indication of successful fabrication. And indeed, with no interlayer present, only 40% of the hollow fiber RO membranes reached a sufficient NaCl retention, indeed showing how difficult it can be to prepare such membranes. Also with an interlayer of just a single PSS coating, the success rates were low, demonstrating that just changing the surface properties from cationic to anionic is not sufficient. However, for both PEM interlayers high success rates were achieved, with especially 3.5 PEI/PSS bi-layers leading to a very high success rate of 90%. We believe that higher success rate of PEI/PSS over PDADMAC/PSS (73%) stems from the layer chemistry. The primary amines in PEI can react with TMC leading to covalent bond formation between the IP layer and the PEM interlayer. For PDADMAC, a quaternary amine, this is not possible. Clearly, applying PEM interlayers prior to IP layer application significantly enhances the reproducibility and success rate of the prepared hollow fiber RO membranes. By filling the support pores with PEMs, the support surface becomes easier to coat. Moreover, the PEM interlayers help to prevent defects from dominating the separation behavior. We stress that the IP recipe and conditions chosen here were based on an optimized recipe for plain hollow fibres. It is likely that even higher success rates can be achieved for the LbL systems when the IP protocol is further optimized.

3.3. Pure water permeability and membrane morphology

With successful hollow fiber RO production established, it becomes important to study the membrane properties in more detail. The pure water permeability of our membranes was measured before and after interfacial polymerization, with the results given in Fig. 5. For these pure water permeabilities, we only took into account the successfully produced membranes with NaCl retention >90% (see Fig. 4). We did measure the water permeability for the defective membranes, but as expected, these were high and highly variable, in line with membranes that contain pinholes.

As can be observed in Fig. 5, plain HF supports show high permeabilities (120 ± 30 L/m^{2}h.bar) that would be expected for tight ultrafiltration membranes. However, when just a single layer of PSS is applied, the permeability drops significantly indicating good adsorption of the polyelectrolyte on and in the membrane pores. For the PDADMAC/PSS and PEI/PSS multilayers, the permeabilities are again significantly lower, in a normal regime for nanofiltration membranes. A

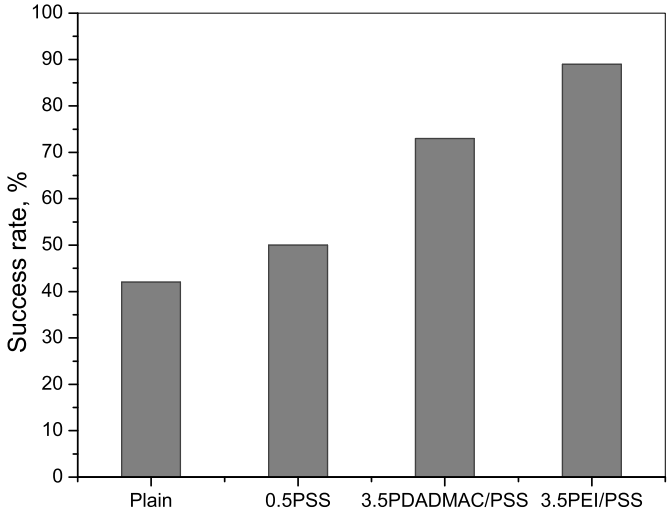

Fig. 4. Success rate of fabricated HF RO membranes according to NaCl retention. For these experiments, at least 10 hollow fiber membranes were produced individually. A membrane was counted as successfully produced when the NaCl retention was higher than 90%.

Table 2
Comparision of NaCl retention and permeability (5 mM NaCl retention under cross-flow velocity and an applied pressure of 5 bar at room temperature).

Membrane	NaCl retention, %	Permeability, L.m^{-2}.h^{-1}.bar^{-1}	Conditions	References
Plain	94 ± 1.7	0.9 ± 0.22	295.5 ppm, 5 bar	This work
0.5 PSS	97 ± 0.6	0.26 ± 0.08		
3.5 PDADMAC/PSS	97 ± 0.6	0.55 ± 0.11		
3.5 PEI/PSS	97 ± 0.7	0.58 ± 0.11		
FilmTech XLE	96.8	2.69 ± 0.25	2000 ppm, 25 bar	[27]
TFC	98.1	8.9	1000 ppm, 10 bar	[14]
mHKUST-1@PA	97.6	6.94	2000 ppm, 4 bar	[15]

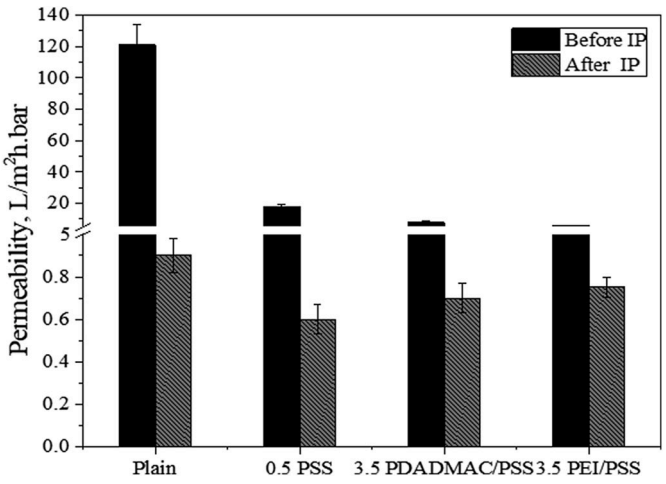

Fig. 5. The change of pure water permeability (PWP) of hollow fibers before and after IP coating.

thicker PEM layer is able to fully close the membrane pores, making the PEM the active separation layer of the membrane [16].

Following the permeability tests of the prepared modules, interfacial polymerization was applied on the lumen (lumen surface) of all hollow fibers and thin film composite (TFC) HF membranes were obtained. The pure water permeability of all successfully fabricated TFC membranes was found to be below 1 L/m^2 h bar (Fig. 5), in line with expectations. The highest permeability values were obtained for the plain supports coated with an IP layer. As expected the PEM interlayer does come at a small cost to the permeability. Partly this is because the PEM layer itself adds an additional resistance to the membrane, but it could also be that PEM interlayers lead to different morphologies for the IP layer. For this reason, we also studied the membrane morphology, before and after coating, by SEM.

The permeability of TFC membranes is often correlated to their surface morphology [10,16,24–30]. In Fig. 6 and Fig. 7, we show surface and cross sectional images of our membranes before and after IP coating. For the polyelectrolyte modified support membranes, the surfaces look the same in all cases, a nice smooth surface. There is evidence of a coating on top of the membrane for both PDADMAC/PSS and PEI/PSS, but the coating is too thin to be characterized, in line with the expected thicknesses based on Ellipsometry (Fig. 2). After IP coating, on all membranes a very clear IP layer is observed. Sharabati et al. studied how the membrane supports pore size can affect the IP layer polymerization and the resulting morphology in relation to RO separation performance [17]. According to their findings, increasing average support layer pore size makes active layer surfaces rougher, with a more pronounced ridge and valley structure and thicker films. Singh et al. demonstrated that TFC membranes with ridge and valley structures typically result in a lower NaCl retention and in defected films [31]. In Fig. 6 we observe that the surface of the IP layer coated directly on our UF support seems to be rougher compared to the 0.5 PSS, 3.5 PDADMAC/PSS and 3.5 PEI/PSS membranes. Indeed a ridge and valley structure is observed for the UF support. In contrast, for the membranes pre-coated with polyelectrolyte layers, and especially for the PEM layers, ear like protuberances were observed, while some small nodular structures can be recognized as well. This difference in layer structure would indeed be expected to lead to small differences in water permeability, as shown in Fig. 5.

3.4. Salt and micropollutants retention of hollow fiber membranes

Finally, we studied the membranes, after IP coating, for their retention of mono and di-valent salts (NaCl, $CaCl_2$ and Na_2SO_4) and for their retention of small organic molecules such as micro-pollutants. As can be clearly seen in Fig. 8, the salt retention of membranes was found to be substantially higher when a PEM interlayer is applied. Moreover, for both the PDADMAC/PSS and PEI/PSS PEM interlayers a higher reproducibility was observed as indicated by the small error bars. These differences could stem from the different surface structures of the IP layers with and without and interlayers as was shown in Table 2. Another likely explanation is that a very small degree of defects (pinholes) is present in the IP layers prepared directly on the UF support, while on the PEM interlayer such defects are prevented. The salt retention values of membranes prepared with just a single PSS layer as interlayer also show good retentions, which can be considered as surprising if we take into account the low success rate of producing these membranes (Fig. 4). The permeability results of salt filtration are also given in Supplementary Fig. S4.

Another difference between the TFC membranes prepared with and without an inter-layer is the relative retention of mono and di-valent salts. For the TFC membrane prepared on a plain support, the retention for the monovalent NaCl and for the di-valent $CaCl_2$ and Na_2SO_4 are nearly equal, while for the TFC membranes with interlayers the di-valent salts are retained more than the monovalent salt. This would again be an indication that the lower salt retention of the plain support based TFC membranes stems from pinholes, while for the interlayer based membranes standard Donnan and di-electric effects lead to higher selectivity for di-valent salts.

Hollow fiber based RO membranes could be highly promising for applications regarding surface water treatment to remove micro-pollutants, but micro-pollutants come in a large variety of properties and sizes. To study the retention of micropollutants (MPs), a cocktail of eight different MPs was assembled containing charged and uncharged (at pH 5.8), but also hydrophilic and hydrophobic MPs of different sizes [16]. The obtained retentions are given in Fig. 9. If we examine the average retention of MPs, it is clear that the retention increases when a PEM interlayer was applied prior to TFC step. Here both PEM based membranes also outperform the single PSS coating based interlayer. It is important to mention here that a change from 96% to 98% average retention might seem just a small change but it represents doubling of the membrane selectivity and thus halves the amount of MP's to be found in the permeate.

4. Conclusion

In this study, we successfully combined PEMs and IP layer on both model surfaces (silicon wafer) and on hollow fiber membranes. Indeed, IP layers can be successfully prepared on PEMs, on layers as thin as a single bi-layer. The thickness of the formed IP layer was found to be independent of the PEM coating thickness, except when going to really thick PEM layers with larger degrees of roughness.

These findings on model surfaces were then used to fabricate hollow fiber based RO membranes. We propose that a PEM can act as an interlayer for the IP layer that acts to prevent the formation of defects, especially pinholes. Moreover, if a pinhole would be formed, the PEM interlayer can prevent the defect from dominating permeability and selectivity by slowing down transport through the pore (analogue to a gutter layer as used in gas separation). This is especially important as hollow fiber RO membranes are very difficult to produce, with defects being common. For IP layers prepared on a plain hollow fiber UF, the success rate was found to be as low as 40%. However by application of a PEM interlayer the success rate increases to 72% for PDADMAC/PSS and 90% for PEI/PSS. We hypothesize that the difference in the success rate between these two systems stems from a difference in chemistry. As PEI has primary amines, the PEI/PSS multilayer can participate in the interfacial polymerization process to form covalent bonds with the IP layer. For PDADMAC/PSS this is not possible as PDADMAC only contains quaternary amines.

In membrane performance the interlayer based membranes have a slightly lower pure water permeability than the plain UF based TFC membranes (0.7 L/m^{2}hbar for the interlayer based membranes, versus

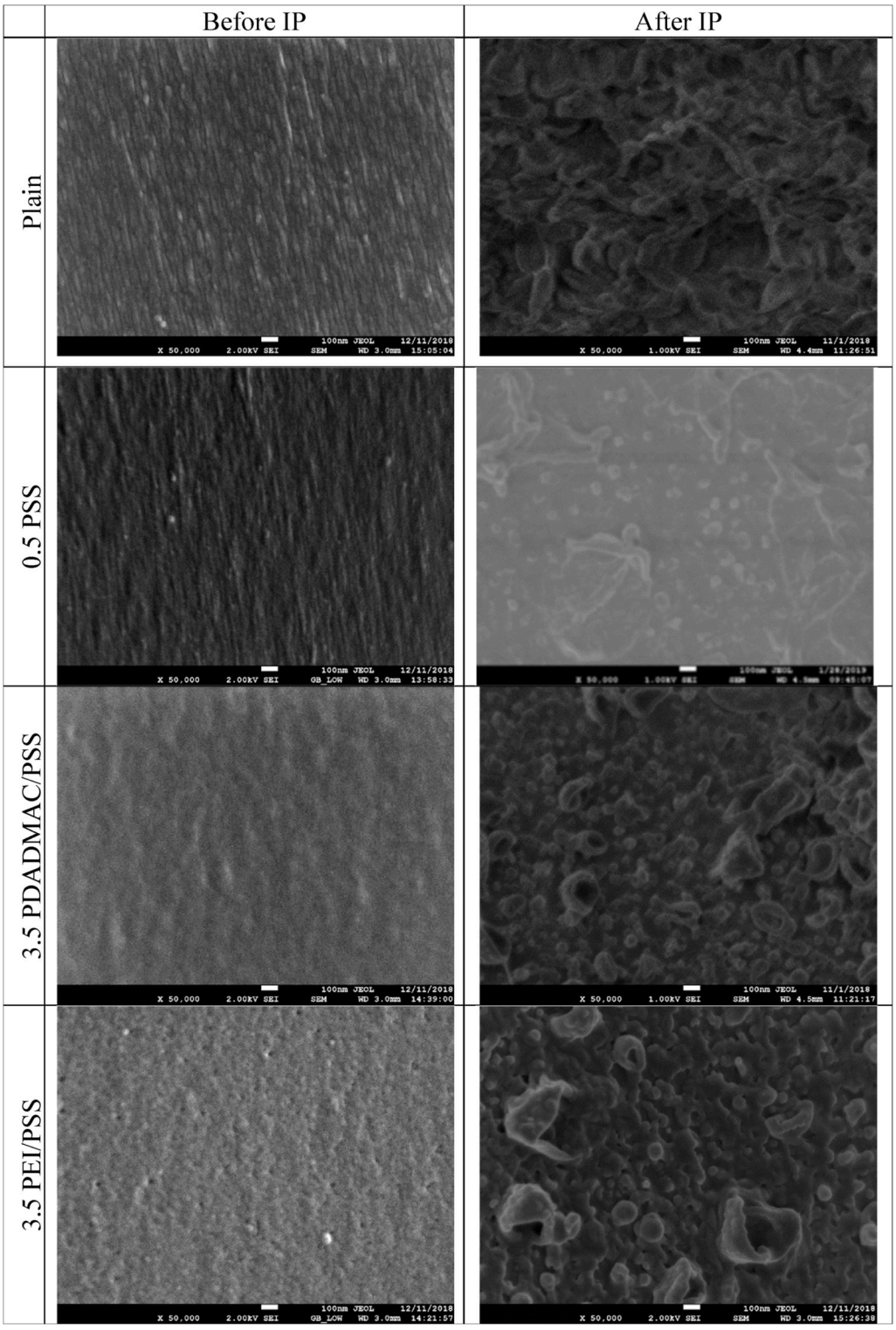

Fig. 6. Lumen surface SEM images of the lumen surface of membranes of hollow fibers before and after IP coating (magnification: 50.000x).

0.9 L/m^{2}hbar for the plain). On the other hand, the separation behavior in both salt retention and micro-pollutant retention is significantly better for the interlayer based membranes. The lower permeability but higher selectivity is expected to stem from a small degree of defects still present in the plain UF based TFC membranes, which are not there or not dominant in the interlayer based membranes. This is supported by morphology studies, where a ridge-valley structure, prone to defects, was observed for the plain UF based membranes, and a more earlike and nodular structure for the interlayer based membranes.

Overall, we show that using a PEM interlayer in the production of hollow fiber RO membranes is highly promising to solve the re-curing problem of defect formation. Especially PEM coatings that can participate in the interfacial polymerization process, such as PEI/PSS, lead to much needed high reproducibility. These hollow fiber RO membranes would be especially promising the remove the remains of medicines and pesticides from waste water and surfaces water, without the current

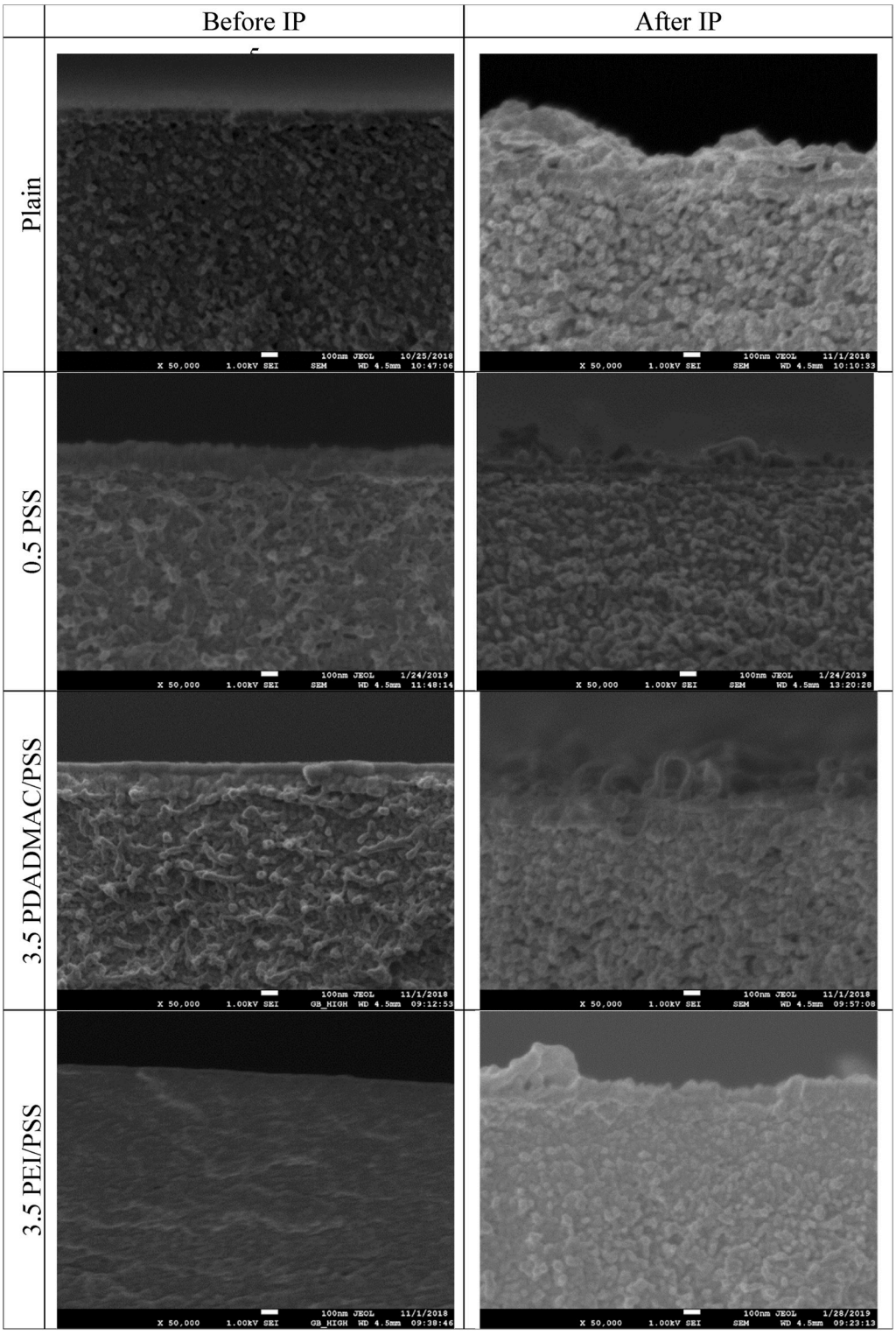

Fig. 7. Cross-sectional SEM images of the lumen surface of membranes of hollow fibers before and after IP coating (magnification: 50.000x).

drawback of spacer fouling found in spiral wound based RO membranes. Still, optimization of the coating conditions will be required to further improve membrane performance. Moreover, this approach would require especially strong HF support membranes to allow operation at high pressures.

Declaration of competing interest

The authors declare no conflicts of Interest.

CRediT authorship contribution statement

Türkan Ormanci-Acar: Conceptualization, Data curation, Investigation, Methodology, Writing - original draft, Funding acquisition.

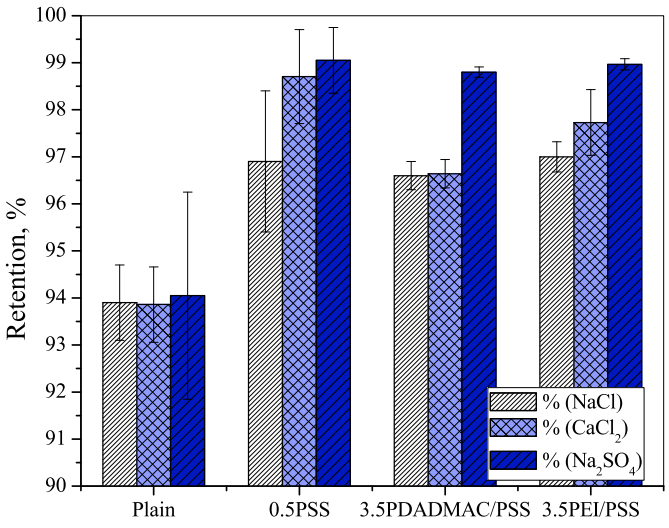

Fig. 8. 5 mM salt retentions results of fabricated HF RO membranes. Retention measurements were performed on at least 5 separately produced membranes under cross-flow velocity and an applied pressure of 5 bar at room temperature. Error bars represent the standard deviation.

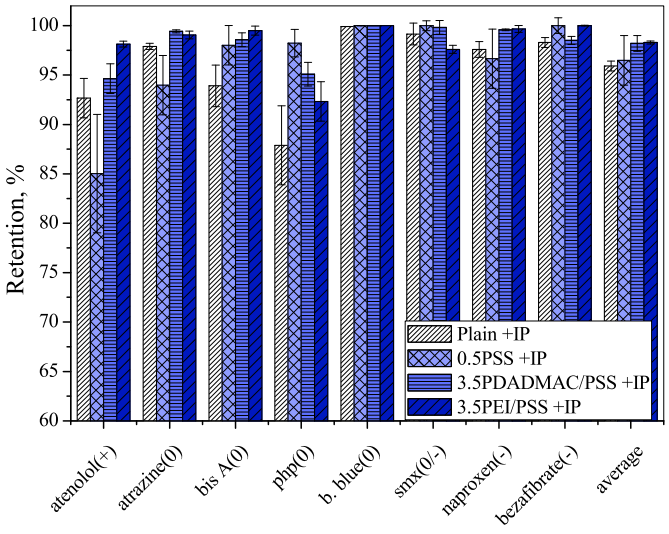

Fig. 9. Micropollutants (MPs) retention results of fabricated HF RO membranes. Retention measurements were performed on at least 5 separately produced membranes under cross-flow velocity and an applied pressure of 5 bar at room temperature. Error bars represent the standard deviation.

Mehrdad Mohammadifakhr: Data curation, Investigation, Methodology, Writing - review & editing. **Nieck E. Benes:** Conceptualization, Supervision, Writing - review & editing. **Wiebe M. de Vos:** Conceptualization, Project administration, Supervision, Writing - original draft, Funding acquisition.

Acknowledgments

This study was supported by the TUBITAK, The Scientific and Technological Research Council of Turkey within the scope of 2219 program (Project No. 1059B191700145). We would like to thank Aquaporin A/S (Lyngby, Denmark) Company for supporting this project financially.

Appendix A. Supplementary data

Supplementary data to this article can be found online at https://doi.org/10.1016/j.memsci.2020.118277.

References

[1] Y. Wada, M. Flörke, N. Hanasaki, S. Eisner, G. Fischer, S. Tramberend, D. Wiberg, Modeling global water use for the 21st century: water Futures and Solutions (WFaS) initiative and its approaches, Geosci. Model Dev. (GMD) 9 (2016) 175–222.
[2] P. Burek, Y. Satoh, G. Fischer, M.T. Kahil, A. Scherzer, S. Tramberend, N. Hanasaki, Water Futures and Solution-Fast Track Initiative, 2016.
[3] S. Chowdhury, M.J. Mazumder, O. Al-Attas, T. Husain, Heavy metals in drinking water: occurrences, implications, and future needs in developing countries, Sci. Total Environ. 569 (2016) 476–488.
[4] M.O. Barbosa, N.F. Moreira, A.R. Ribeiro, M.F. Pereira, A.M. Silva, Occurrence and removal of organic micropollutants: an overview of the watch list of EU Decision 2015/495, Water Res. 94 (2016) 257–279.
[5] European Commission (Ec), Priority Substances and Certain Other Pollutants (According to Annex II of the Directive 2008/105/EC), 2008.
[6] B. Kasprzyk-Hordern, D.R. Baker, Enantiomeric profiling of chiral drugs in wastewater and receiving waters, Environ. Sci. Technol. 46 (3) (2012) 1681–1691.
[7] S.J. Khan, L. Wang, N.H. Hashim, J.A. Mcdonald, Distinct enantiomeric signals of ibuprofen and naproxen in treated wastewater and sewer overflow, Chirality 26 (11) (2014) 739–746.
[8] B. Petrie, R. Barden, B. Kasprzyk-Hordern, A review on emerging contaminants in wastewaters and the environment: current knowledge, understudied areas and recommendations for future monitoring, Water Res. 72 (2015) 3–27.
[9] S. Theepharaksapan, C. Chiemchaisri, W. Chiemchaisri, K. Yamamoto, Removal of pollutants and reduction of bio-toxicity in a full scale chemical coagulation and reverse osmosis leachate treatment system, Bioresour. Technol. 102 (9) (2011) 5381–5388.
[10] A.K. Ghosh, E.M. Hoek, Impacts of support membrane structure and chemistry on polyamide–polysulfone interfacial composite membranes, J. Membr. Sci. 336 (1–2) (2009) 140–148.
[11] M. Elimelech, W.A. Phillip, The future of seawater desalination: energy, technology, and the environment, Science 333 (6043) (2011) 712–717.
[12] V. Freger, Nanoscale heterogeneity of polyamide membranes formed by interfacial polymerization, Langmuir 19 (11) (2003) 4791–4797.
[13] J.S. Vrouwenvelder, D.G. Von Der Schulenburg, J.C. Kruithof, M.L. Johns, M.C. M. Van Loosdrecht, Biofouling of spiral-wound nanofiltration and reverse osmosis membranes: a feed spacer problem, Water Res. 43 (3) (2015) 583–594.
[14] Y. Zhang, L. Yang, K.P. Pramoda, W. Gai, S. Zhang, Highly permeable and fouling-resistant hollow fiber membranes for reverse osmosis, Chem. Eng. Sci. 207 (2019) 903–910.
[15] Y. Lin, Y. Chen, R. Wang, Thin film nanocomposite hollow fiber membranes incorporated with surface functionalized HKUST-1 for highly-efficient reverses osmosis desalination process, J. Membr. Sci. 589 (2019), 117249.
[16] J. de Grooth, R. Oborný, J. Potreck, K. Nijmeijer, W.M. de Vos, The role of ionic strength and odd–even effects on the properties of polyelectrolyte multilayer nanofiltration membranes, J. Membr. Sci. 475 (2015) 311–319.
[17] J.A.D. Sharabati, S. Guclu, S. Erkoc-Ilter, D.Y. Koseoglu-Imer, S. Unal, Y. Z. Menceloglu, I. Ozturk, I. Koyuncu, Interfacially polymerized thin-film composite membranes: impact of support layer pore size on active layer polymerization and seawater desalination performance, Separ. Purif. Technol. 212 (2019) 438–448.
[18] J.E. Gu, S. Lee, C.M. Stafford, J.S. Lee, W. Choi, B.Y. Kim, J.H. Lee, Molecular layer-by-layer assembled thin-film composite membranes for water desalination, Adv. Mater. 25 (34) (2013) 4778–4782.
[19] J.E. Gu, J.S. Lee, S.H. Park, I.T. Kim, E.P. Chan, Y.N. Kwon, J.H. Lee, Tailoring interlayer structure of molecular layer-by-layer assembled polyamide membranes for high separation performance, Appl. Surf. Sci. 356 (2015) 659–667.
[20] W. Choi, J.E. Gu, S.H. Park, S. Kim, J. Bang, K.Y. Baek, J.H. Lee, Tailor-made polyamide membranes for water desalination, ACS Nano 9 (1) (2015) 345–355.
[21] W. Choi, S. Jeon, S.J. Kwon, H. Park, Y.I. Park, S.E. Nam, E.P. Chan, Thin film composite reverse osmosis membranes prepared via layered interfacial polymerization, J. Membr. Sci. 527 (2017) 121–128.
[22] J.C. Dijt, M.C. Stuart, G.J. Fleer, Reflectometry as a tool for adsorption studies, Adv. Colloid Interface Sci. 50 (1994) 79–101.
[23] J. de Grooth, D.M. Reurink, J. Ploegmakers, W.M. de Vos, K. Nijmeijer, Charged micropollutant removal with hollow fiber nanofiltration membranes based on polycation/polyzwitterion/polyanion multilayers, ACS Appl. Mater. Interfaces 6 (19) (2014) 17009–17017.
[24] Y. Niebel, M.D. Buschmann, M. Lavertu, G. De Crescenzo, Combined analysis of polycation/ODN polyplexes by analytical ultracentrifugation and dynamic light scattering reveals their size, refractive index increment, stoichiometry, porosity, and molecular weight, Biomacromolecules 15 (3) (2014) 940–947.
[25] W. Ogieglo, H. Wormeester, K.J. Eichhorn, M. Wessling, N.E. Benes, In situ ellipsometry studies on swelling of thin polymer films: a review, Prog. Polym. Sci. 42 (2015) 42–78.
[26] J.B. Schlenoff, S.T. Dubas, Mechanism of polyelectrolyte multilayer growth: charge overcompensation and distribution, Macromolecules 34 (3) (2001) 592–598f.
[27] D. Dolar, K. Košutić, B. Vučić, RO/NF treatment of wastewater from fertilizer factory—removal of fluoride and phosphate, Desalination 265 (1–3) (2011) 237–241.

[28] S. Yüksel, N. Kabay, M. Yüksel, Removal of bisphenol A (BPA) from water by various nanofiltration (NF) and reverse osmosis (RO) membranes, J. Hazard Mater. 263 (2013) 307–310.
[29] M.N. Fini, H.T. Madsen, J. Muff, The effect of water matrix, feed concentration and recovery on the rejection of pesticides using NF/RO membranes in water treatment, Separ. Purif. Technol. 215 (2019) 521–527.
[30] G.M. Geise, H.B. Park, A.C. Sagle, B.D. Freeman, J.E. McGrath, Water permeability and water/salt selectivity tradeoff in polymers for desalination, J. Membr. Sci. 369 (1–2) (2011) 130–138.
[31] P.S. Singh, S.V. Joshi, J.J. Trivedi, C.V. Devmurari, A.P. Rao, P.K. Ghosh, Probing the structural variations of thin film composite RO membranes obtained by coating polyamide over polysulfone membranes of different pore dimensions, J. Membr. Sci. 278 (1–2) (2006) 19–25.